Modeling Statistics of Fish Patchiness and Predicting Associated Influence on Statistics of Acoustic Echoes

Daniel Grunbaum
School of Oceanography
University of Washington
Seattle, WA 98195-7940
Email: grunbaum@ocean.washington.edu

Thomas C. Weber
Center for Coastal and Ocean Mapping
Jere A. Chase Ocean Engineering Laboratory
University of New Hampshire
Durham, NH 03824
Email: weber@ccom.unh.edu

Award Numbers: N000141110149 / N000141110151

Note: this is a combined final report for Grunbaum and Weber, and is intended to augment the final report by Tim Stanton under Award Number N00014-11-1-0147 submitted in December 2014.

LONG-TERM GOALS

To accurately describe the statistics of acoustic echoes due to the presence of fish, especially in the case of a long-range active sonar. Toward this goal, fundamental advances in the understanding of fish behavior, especially in aggregations, will be made under conditions relevant to the echo statistics problem.

OBJECTIVES

To develop new models of behavior of fish aggregations, including the fission/fusion process, and to describe the echo statistics associated with the random fish behavior using existing formulations of echo statistics.

APPROACH

Several interrelated components of research were conducted in parallel and in a synergistic way: One important component of this research was the development of new advanced models of fish behavior inspired by, and grounded by, 3-D images of fish aggregations. These images were derived by multi-beam acoustic systems. Key parameters observed and modeled were the rate of fission/fusion of the aggregations and the behavior of fish groups in terms of their trajectories and their characteristic scales. The intent for the observed and modeled fish behaviors was to incorporate them into an existing general formulation for echo statistics.

This effort was a group effort led by Stanton (see the final report for N00014-11-1-0147 from December 2014). This final report focuses on the work of Weber, who analyzed high-frequency (~100 kHz) multibeam echosounder backscatter collected over fish aggregations to parameterize the behavior of fish groups, and that of Grunbaum, who developed new fish behavior models with parameters taken in part from data analyzed in this project. This work involved informal collaborations with Chris Wilson of NOAA Alaska Fisheries, whose team collected the multibeam data, and Ben Jones of NPS who used some of the empirical fish data analyzed by Weber in a forward acoustics model.

WORK COMPLETED

Major milestones were reached in all components of the project--- a new model for fish behavior was developed, optimized for numerical efficiency, and used to make predictions with empirical parameters; 3-D observations of fish schools made with multi-beam sonars and analyzed to determine of important aspects of fish dynamics; and predictions were made of echo statistics of a long-range sonar in a realistic ocean waveguide with fish present. Results from this project have been presented at scientific conferences and are summarized in six scientific papers (three published,two more submitted to refereed scientific journals, and one more in preparation.) In addition, some of the fundamental scientific results were transitioned in a concurrent applied program (ONR HiFAST FNC program) to both NAVSEA and NAVAIR sonar trainers.

The scientific results are given in detail in the following sections.

1. New model for fish school behavior

A novel approach was created in this project towards understanding fission, fusion, and migration of social groups (fish, in this case) by assuming a high level of sensory and cognitive function by interacting individuals. We published the following paper summarizing the results: Grunbaum (2012). Simulations based on this model show all of these behavioral aspects, as illustrated in the time series of fish distribution in Figure 1.

Nearly all current models of social interaction are “zone models" which assume that characteristics of animal groups such as schools, swarms and flocks arise from individuals' immediate responses to the relative positions and velocities of a small number of nearest neighbors. While there is little question that position- and velocity-dependent responses are crucial to social grouping, current zone models commonly predict that large groups (that is, groups in which individuals in different parts of a group must interact indirectly through many individuals between them) should be fragile and therefore rare or transient. However, natural groups are frequently large and stable. In other settings, natural populations that are sparse or distributed in numerous small groups nonetheless maintain common orientation across groups. In most current zone models, directionality can be maintained only by frequent encounters between individuals and groups, and so is unlikely in sparse populations at reasonable levels of behavioral and physical random forcing.

The new model assumes an additional cognitive layer in fish schooling behavior, in which encounters with neighbors are used as input data on which to base statistical estimates of the density and movement characteristics of the local population. The key idea is that each individual is continuously updating its understanding of the intent of its neighbors, and basing its own decision-making on this understanding. Thus, social individuals can glean information even when the instantaneous position and velocity of neighbors are quite different from overall movement patterns, or when neighbors are so sparse that encounters with them are rare.

The above line of reasoning suggests a new hybrid model that combines agent-based "Lagrangian" movement rules with a "Eulerian" distribution of population density and flux, together with local distributions of orientation angle. This hybrid approach has multiple advantages from the perspective of understanding acoustic signatures of fish in real-world settings. One is computational tractability: Agent-based models of social grouping are inherently N^2 computations, where N is the number of individuals. (Specifying maximum interaction distances can enable subdivision of the habitat into non-interacting parts, but computational requirements remain large for dense groups.) The hybrid model executes parallel simulations, in which the estimates of local population characteristics evolve as partial differential equations, and the individuals respond to estimates as autonomous agents. Hence, there is no N^2 calculation required. Another advantage of our hybrid approach is that the statistical distributions calculated during social simulations (population density, orientation angles, etc.) are directly relevant to estimates of acoustic signatures.

The hybrid modeling assumes a Bayesian framework for local estimation of population movement. For example, for estimates of local density, we assume each individual maintains a Bayesian updating scheme for determining the expected value and uncertainty associated with the Poisson distribution of neighbors. In a standard updating scheme, appropriate for statistically stationary neighbor distributions, the uncertainty decreases monotonically with ongoing sampling. In application to schooling, in which populations move and therefore are not statistically stationary, we discount the predictive value of old information. Hence, an individual's uncertainty about local density and direction fluctuates downwards when informative samples occur frequently and upwards when such samples are rare.

2. Parameterizing and optimizing new model for fish school behavior

This work followed the above development (Section 1) of the new fish schooling model and focused on estimating parameters of the new model using individual-level and population-level fish schooling data. The individual-level data are 10-minute-long 3-dimensional-trajectory sequences of all individuals within small schooling and milling aggregations in the laboratory. The population-level data were collected in field surveys of Alaska pollock being analyzed by Weber and Stanton as described below in Section 3. The model and its application to schooling analysis involve a relatively large number of parameters, which must be constrained and optimized with respect to the available data. Therefore, much of the effort also involved building computational and statistical machinery to execute this optimization. Both the number of parameters and the relatively high computational demands of large-scale spatially-explicit schooling models make effectiveness and efficiency key to successful parameter-fitting. The principal modeling accomplishments, specific to parameterizing and optimizing, are summarized:

(a) We reanalyzed individual-level fish trajectory data to comprehensively characterize individual positions and movements within groups and to quantify neighbor-neighbor turning and acceleration responses. We developed new computational machinery for parameter-fitting behavioral models to our individual-level fish trajectory data. We conducted large-scale numerical optimization to obtain best-fitting behavioral response zones for short-memory cases. We have also extended our analysis to long-memory cases. We conducted simulations using the best-fit behaviors to assess the degree to which they reflect the observed behaviors from which they were extracted.

(b) We developed model computer code to embed observed fish trajectories into the new cognitive schooling model. This enables us to conduct simulations in which modeled fish respond to actual observed fish behavior. This also enables us to assess model behaviors by replacing one

or more members of a real fish aggregation with a simulated counterpart, and quantifying the degree to which position, movement and neighbor-neighbor responses are statistically consistent with the true behavior.

(c) We developed model computer code to identify and characterize schools in the output of the cognitive schooling model (Fig. 2). Identification of schools is based largely on mathematical morphology analysis techniques for "segmentation" of features in images. Densities and edge characteristics of groups are used to delineate them from surrounding non-group distributions. This analytical machinery is a key tool in constraining model parameters to field surveys of fish schools that quantify distributions of group size, shape and separation distance.

(d) We developed computational infrastructure to extract cognitive behavior and other parameters from the NOAA Alaska Fisheries Science Center acoustic/trawl walleye pollock survey data. The central challenge in parameter estimation from data of this type is that data have incomplete spatial coverage and, at any given spatial position, are irregular in time. A consequence is that, within a set of repeated surveys, each acoustic transect reflects an unknown fraction of fish that were previously detected, that moved into the survey area since the last transect, or that left the survey area since the last transit.

Our approach to estimating parameters utilizes iterated simulations of behavioral models, maximizing statistical similarities between predicted and observed data where observations are available. The gist of this approach is that a model provides a means to accumulate information between intermittent and probably sparse data. The combination of data and movement mechanisms embedded in the equations enable the model to "learn" as much as possible about the state of the system. A necessary element in this maximization is as unbiased as possible a "null" population distribution for areas in which no observation data are available. Because in this dataset the speed and direction of ambient currents is not known, the analysis is implemented in two steps. The implementation of both stages of analysis is derived from the cognitive schooling behavioral model developed in this project. In the initial step, ambient current velocity is inferred by maximizing "fit" of observed fish densities over time and space using the entire acoustic times series. In this step, current velocity is assumed to be constant within a given depth stratum. In the second step, the spatial map of localized fish group velocities at each time/space coordinate in the domain of interest is inferred by maximizing the "fit" of model projections with acoustic observations. The result is a statistical "best estimate" of the swimming velocities of fish at every point in time and space informed by the acoustic surveys.

An example of this method is given in Fig.s 3 and 4. Fig. 3 shows first-stage ambient current velocity estimates for the walleye pollock survey data using a constant coefficient advection-diffusion process as the underlying movement mechanism for fish populations. The analysis goes through the entire sequence of recent surveys, and determines the advection velocity and diffusion that yield the best matches between model and data (according to one of a number of statistical metrics; the figure reflects a likelihood metric). Because the input data include all acoustic returns (not just above-threshold returns indicating dense fish aggregations), the best-fit advection velocity for fish signals likely is dominated by the ambient current velocity. The diffusion coefficient reflects movement and fission/fusion of fish schools, possibly with contributions from other sources. Fig. 4 shows the second stage analysis, in which the estimated current velocity is used to quantify how the fish are moving relative to the water in

which they are immersed, reflecting the best fit estimates of true school movement dynamics as schools move, split and fuse across time and space.

(e) Because cognitive schooling models have not been developed previous to this project, statistical methods for estimating cognitive behavioral parameters do not yet exist. To develop statistical tools for inferring these parameters, we considered a simpler spatial memory/cognition problem, which is the odor source location problem, applicable to many engineering and environmental problems of interest to the Navy. We had access to trajectories of male moths finding a pheromone-emitting female; our goal was to quantify the mate-seeking behavior of these male moths in a cognitive behavioral framework. This is a simpler parameter estimation problem because ways in which the geometry of plumes transported by turbulent environmental flows might be statistically summarized are known from fluid physics.

Using the moth dataset, we developed new biomimetic cognition-based algorithms for odor source location, and mapped out strategies for estimating parameters of models of spatial memory and cognition (Fig 5). We assumed that cognitive parameters were structured so as to estimate and respond to plume geometry in the most efficient way. The guidance to parameterizing behavioral parameters provided by this assumption was central to obtaining parameter estimates that explain large fractions of variance in observed movements. This work is described in a manuscript in collaboration with a chemosensory ecologist and was submitted to the Journal of Movement Ecology (Grunbaum and Willis, 2014). As with fish schooling, this is an entirely new approach to assessing this biological phenomenon, which will be stimulating and useful to a wide range of future investigations.

3. Inferring fish school characteristics from seabird foraging behaviors

Foraging seabirds are highly informative about fish distributions and schooling behaviors, both directly as model systems of social grouping and information sharing, and indirectly as rapidly-responding indicator of location, abundance, size, depth, species and other characteristic of prey schools. For foraging seabirds, effective search strategies can make the difference between breeding success and failure; hence, strong natural selection is expected for optimal use of information, especially when prey is concentrated in schools. Seabirds are hypothesized to utilize cognition to gain up-to-date information on fish school distributions by monitoring the direction of birds returning to the colony or the behavior of other birds at sea through network foraging. However, search strategies based on this type of social information is affected by seabird population densities. We used Bayesian analysis of Peruvian anchoveta (*Engraulis ringens*) in the northern Humboldt Current System to generate simulated fish school distributions with the differing spatial structures observed in two years, 2008 and 2009 (Fig. 6). We analyzed movement data of Peruvian Boobies (*Sula variegata*) to extract parameters for a spatially-explicit individual-based foraging model. We then used the model to assess how variations in foraging trip statistics reflect differences in fish school distributions. We simulated a range of scenarios, including ranges of seabird population densities and different weighting of alternative types of information available to seabirds before embarking on foraging trips. In our simulations, orientation of outbound headings in line with returning birds enabled departing birds to avoid areas without prey even at relatively low population densities (Fig. 7). The mechanisms underpinning network foraging become more effective as population densities increase and may be facilitated by other search strategies that concentrate individuals in profitable areas. These results, presented in Boyd et al. (in prep.) suggest that monitoring seabird foraging behaviors at colonies, specifically the time and direction of departures on foraging trips, is a potentially effective approach to assessing both large-scale distributions of fish schools and more detailed characteristics such as depth, size and species composition.

4. Extracting fish-behavior parameters from high resolution images of fish aggregations derived from acoustic multibeam data

Multibeam data analysis has focused on data collected in the Eastern Bering Sea (EBS) during both 2010 and 2012. These data were collected using a Simrad ME70 multibeam echosounder as part of the NOAA Alaska Fisheries Science Center (NOAA-AFSC) acoustic/trawl walleye pollock surveys. Through use of sequential pings from the 2-D multibeam data, 3-D images of fish schools could be made (Figs. 8-9).

Data collections from both years represent multiple (approximately 9) week survey efforts aimed at broad-scale stock assessments in the EBS, and ME70 data have been made available to this project courtesy of Chris Wilson (NOAA-AFSC). Most of the data were collected along widely spaced (~40 km) transects, and for the purposes of this research are considered to represent a 'snapshot' of the pollock aggregations present in the EBS. These widely spaced transects from 2010 were analyzed to form clusters of volumetric backscatter representing mid-water pollock aggregations (Figure 8). 49,650 clusters were extracted over an 8 day period, and compared to the general models of Anderson [1981] and Niw [2003]. The data can be fit to the Anderson [1981] model.

During the 2012 data collection effort, NOAA-AFSC also conducted repeat transects at our request and with our guidance on two occasions. This resulted in ~1-nmi-long transects that were repeated every 10-15 minutes, with 24 transects on the first occasion and 14 transects on the second occasion. Analysis of the 2012 data concerned studying rates of schooling fission and fusion. These latter data were analyzed to extract metrics describing morphological changes in the fish aggregations that can be used to tune or ground-truth behavioral models. Metrics of particular interest include group scales for length, velocity, and time, trajectories of individual groups, and bounds on the rate at which aggregations appear to split (a 'fission' event) or recombine (a 'fusion' event). Data of these type (repeat passes over the same groups) provide a unique observation of group dynamics at a local scale, although they are rarely collected. A manuscript describing these data has been submitted (Weber, 2015).

Statistics of fish school size—population level

To examine the statistics of walleye pollock, an automated process was generated and exercised for the ME70 multibeam echosounder data. Eight days of survey effort in July 2010 were analyzed to form clusters of volumetric backscatter representing mid-water pollock aggregations (Figure 11). These data cover a region extending from 176ºW to 179.5ºW and 58ºN to 62.5ºN. Mid-water trawls (N = 43) conducted in this region caught 98% pollock by weight. The ME70 data were processed to

a. remove potential seabed returns and sidelobe contamination
b. remove data below a threshold of Sv = -60 dB (independent of beam angle)
c. remove spatially isolated targets that are considered 'speckle' noise
d. cluster, and uniquely label, data that are within 25 m of each other horizontally and 5 m of each other vertically
e. extract metrics describing each cluster including the cluster volume,V, maximum vertical extent, H, and maximum horizontal extent, L.

This process resulted in 49,650 clusters of fish were extracted for the 8 day period. Histograms of their effective size, $V^{1/3}$, vertical extent, and horizontal extent are shown in Figure 12. Also shown are best fits of the data to the models of Anderson [1981] and Niwa [2003]. Neglecting issues that may arise from the ME70 finite field of view and range/angle-dependent resolution, the data suggest that the pollock aggregations have a high aspect ratio: the mode of the horizontal extent is approximately 6 times greater than the mode for the maximum vertical extent. The data can be fitted quite closely to the Anderson model, which assumed disk-like aggregations of fish and modeled the diameter of schools.

Observations of fish group behavior at the local level

An important caveat in the population statistics shown in Figure 12 is that the data represent aggregations of both juveniles and adults, nighttime and daytime behaviors, other environmental covariates, and possible 'contamination' from other species. To examine this issue further, we have extracted population statistics from the 2012 repeat transects. The first set of repeat transects targeted small, dense fish aggregations ("cherry balls") that were fully contained within the ME70 field of view. The second set of repeat transects targeted dense aggregations that could be acoustically mapped, but which at least partially extended outside of the field of view. For the first set of repeat transects (Figure 11), the fish aggregations observed on consecutive passes appeared to be uncorrelated, and were largely constrained to dense aggregations at water depths less than 80 m with a large, widely-spaced aggregation of targets below 80 m. The second set of repeat transects exhibited dense aggregations of fish throughout the water column, with a quasi-continuous distribution of fish below 80 m water depth and relatively well-separated aggregations in the upper portion of the water column (Figure 12). These data were processed similarly to the 2010 ME70 data, except that rather than cluster the data based on an a priori assumption about horizontal and vertical 'linking' distances, the data were contoured based on volume scattering strength. Aggregation metrics were subsequently calculated at the contour level representing a fish density 100x less than the peak density. This approach made it possible to treat discrete and quasi-continuous aggregations using the same methodology. The distribution of the effective school horizontal radius is shown in Figure 13 for the 1st set of repeat passes ('subset 1'), and for the second set of repeat passes for fish observed in the upper 80 m of water ('subset 2, upper 80 m'), below 80 m ('subset 2, below 80 m'), and for a 10 m thick layer between 90-100 m ('subset 2, 90-100 m'). Each distribution appears quite similar and, like the larger population of aggregations analyzed from the 2010 data, fit a power-law distribution of approximately L^{-3} for the larger aggregation sizes.

The repeat-transect data collected in 2012 were further analyzed to extract group behavioral metrics with the express goal of using them to iteratively fine-tune fish behavior models. First, a subset of the passes corresponding to the time before sunset (at which time the general behavior of the fish was observed to change) was used (Figure 14). Where possible, fish detections that appear to be jointed during any one transect were tracked as they moved and underwent fusion or fission events. An example of this process is shown in Figure 15. For the first two passes (A and B) shown in Figure 15, the group exhibited approximately the same volume and volume scattering strength, S_v. The group then split into two subgroups over the subsequent passes (C1, C2 and D1, D2). The subgroups appear to recombine during the fourth and fifth passes, and remained together through the sixth pass. The combination of S_v and volume data are consistent enough to suggest that it is possible to follow a large fraction of the group from transect to transect, offering a rare glimpse of fish group fusion and fission events. The S_v data and the TS to length model of Traynor (1996) together with the frequency response work of de Robertis et al [2010] suggest that the average spacing between fish is 1.5-2.0 m throughout the six transects.

We have also determined several other group parameters for fish groups that were identified in sequential passes. For example, The group speed, V_g, is found by computing the horizontal distance traveled and dividing by the time between observations. A characteristic group length scale, L_g, for each pair of observations is found by taking the cube root of the average of the volumes for the sequential passes. A group time scale is then found from $T_g=L_g/V_g$. This resulted in N=19 observations of group length scales, group velocities, and group time scales (Figure 16). The average L_g, V_g, and T_g are 31 m, 5 cm/s, and 770 seconds, respectively. The small sample size makes it difficult to unambiguously empirically fit statistical distributions to these data. For each parameter, however, the data more frequently lie below the mean: the median is generally 15-30% lower than the mean. There is no apparent correlation (r = 0.1) between L_g and V_g.

These results were presented in a special session on fish acoustics in the Spring 2014 scientific meeting of the Acoustical Society of America in Providence, R.I. A manuscript based on the final results described here has been submitted (Weber, 2015).

RESULTS

We have reached major milestones of new understanding in two complementary areas: **1. Modeling of fish behavior.** The advanced modeling of fish behavior has yielded significant results. Fission, fusion, and migratory behavior of the fish have been modeled. These results use a hybrid approach that integrates both intelligence of the fish in nearest neighbor interactions as well as group behavior. Modeling of 3-D data has given information on the rate at which fish exit a school. Through use of empirical parameters and numerical optimization, realistic predictions of fish behavior have been made. **2. 3-D sonar observations of fish schools.** (a) Examination of data from several locations in the world has consistently exhibited a mode in the statistics of school dimensions, which provides information for the modeling in #1 above. (b) Time series data from repeated passes of fish has provided a rare ocean investigation of fission/fusion processes yielding critical empirical information on fish dynamics in their natural environment. For example, the speed at which groups of various sizes move, split, and recombine, is rarely observed outside of laboratory settings. These data help to bound the space/time scales at which information is passed (or remains coherent) within the school. These group-level ocean data, coupled with our laboratory data involving individual fish, are being instrumental in enabling the model (through experimental parameterization) to make realistic predictions.

In addition, a closely associated effort led by Stanton provided integration of these two milestones with the **echo statistics from a long range sonar in the presence of fish schools**. This effort demonstrated that echo PDF's from fish schools are heavy-tailed, and the degree to which the tail of the echo distribution is non-Rayleigh depends directly upon the number of patches of fish in the sonar beam. Consequently, the level of the tail is dependent both on the population statistics of the fish in general, and on the local, within-beam behaviors of the fish groups.

Overall, the combination of the new modeling and measurements of fish schools, along with the predictions of echo statistics associated with long-range sonars, provides a powerful suite of tools to make realistic predictions of long-range sonar performance in the presence of fish and under a wide range of realistic conditions.

IMPACT/APPLICATIONS

The modeling and observations of fish behavior represent an advancement of the fundamental understanding of fish behavior. A key advancement in the modeling is including fish "intelligence". Integrating the 3-D ocean data with the model is creating a powerful tool for making realistic predictions of fish behavior. The modeling of echo statistics from a mid-frequency sonar with fish aggregations present demonstrates the fish clutter characteristics relevant to Navy ASW applications. The observed speeds of fish schools yields information on the degree to which fish impact Doppler-sensitive sonars. The advanced behavior model is in a form that can be incorporated into the echo statistics model. The combination of the two models, grounded by our observations of fish behavior, provides a significant tool for predicting sonar performance associated with the presence of fish.

TRANSITIONS

The 3-D fish shoal data, provided by NOAA Fisheries and analyzed in this project, were the basis (credit due to Stanton) for a transition of the biologic simulations in the HiFAST FNC ONR program (LaCour, Stanton, Jones) to the CASE (NAVAIR) sonar trainer. In addition, transition of the shoal data into the SAST ACB15 (NAVSEA) sonar trainer via the HiFAST program has been approved and is currently being incorporated into the system at the time of this writing.

RELATED PROJECTS

Parts of this project fed into the concurrent ONR HIFAST FNC program (LaCour, Stanton, Jones) in which fish echoes were simulated for use in Navy sonar trainers (SAST-NAVSEA and CASE-NAVAIR) (see "Transitions" above). The 3-D multi-beam data involving fish shoals from the Eastern Bering Sea, provided by NOAA Fisheries and analyzed in this project, were used in the HiFAST program to predict echoes from shoals.

PUBLICATIONS (Refereed)

Grunbaum, D. (2012) A spatially explicit Bayesian framework for cognitive schooling behaviors. Interface Focus. doi: 10.1098/rsfs.2012.0027 [published, refereed]

Grünbaum, D. and M. A. Willis. (2015) Spatial memory-based behaviors for locating sources of odor plumes. Movement Ecology. Movement Ecology 3:11 [published, refereed].

Jones, B.A., J.A. Colosi, and T.K. Stanton (2014), "Echo statistics of individuals and aggregations of scatterers in the water column of a random, oceanic waveguide," J. Acoust. Soc. Am., DOI 10.1121/1.4881925 [published, refereed]

Stanton, T.K., Bhatia, S., J. Paramo, and F. Gerlotto (submitted), "Comparing modeled group size distributions to 3-D multibeam sonar data on fish school dimensions," Can. J. Fish. Aq. Sci. [submitted, refereed]

Boyd, C., D. Grünbaum, G. Hunt, A. E. Punt, H. Weimerskirch and S. Bertrand (2015) Effectiveness of search strategies used by foraging seabirds to locate pelagic prey. Behavioral Ecology [in prep., refereed]

Weber, T. and D. Grunbaum, (2015), "Observations of group behavior in walleye pollock (*Gadus chalcogrammus*)," ICES J. Mar. Sci. [submitted, refereed].

Fusion-fission dynamics model for fish school behavior

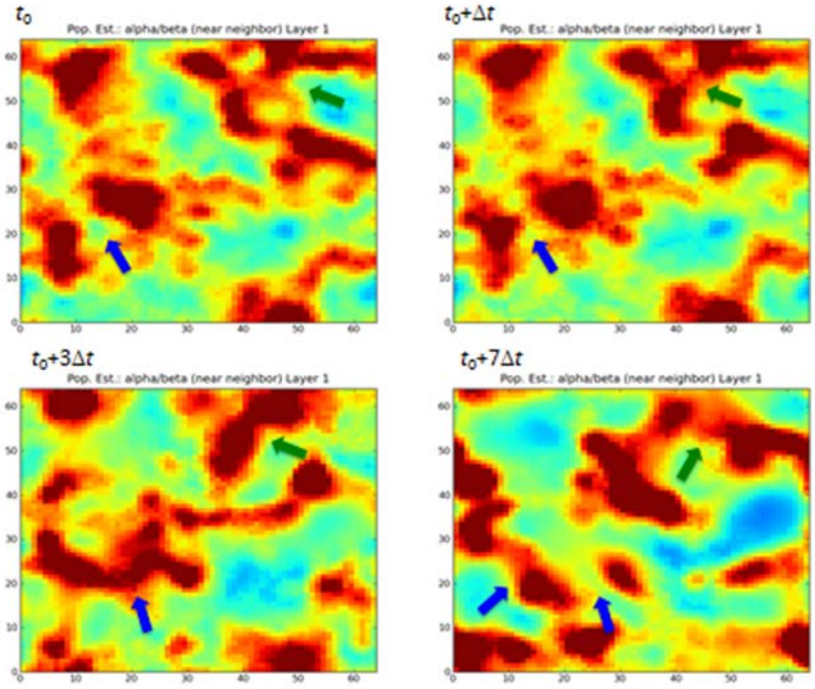

Figure 1. Fission-fusion dynamics in the cognitive schooling model, reflected in population-level density distributions at four sequential time steps (note varying time increments between images). Blue arrows indicate approach and then fusion of two groups, followed by a subsequent fission event and incipient fusion with another group. Green arrows indicate a simultaneous approach/fusion/fission sequence in a different part of the simulation domain. Computations using new model published in Grunbaum (2012).

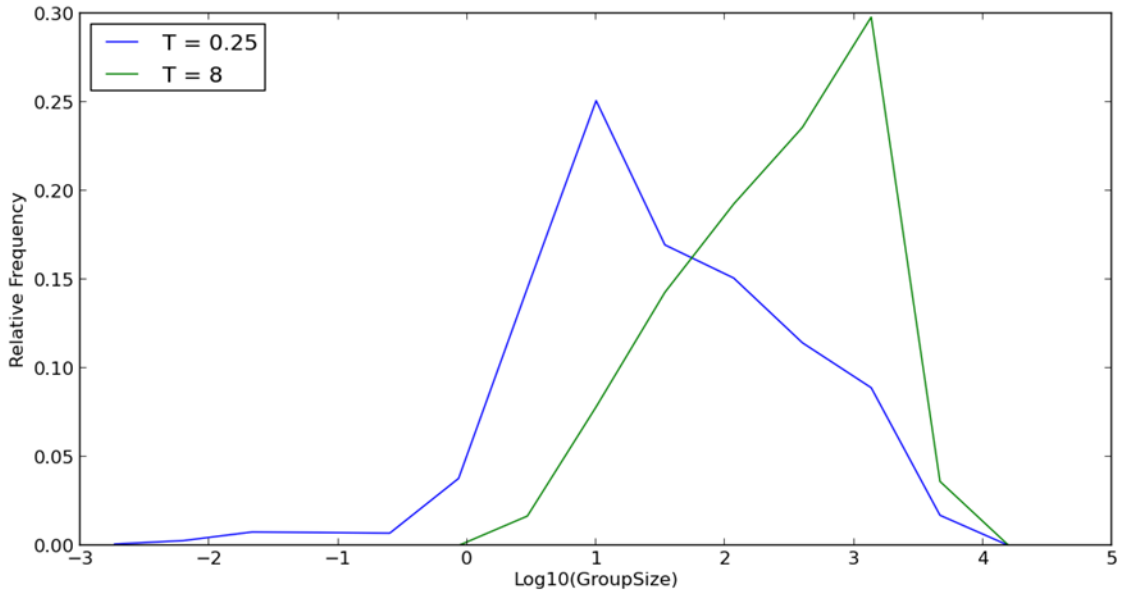

Figure 2. An example of group size distributions from school segmentation in the cognitive schooling model using mathematical morphology techniques. Size is quantified as the total number of fish within separate schools. Units are arbitrary (rescaled and nondimensionalized from physical units). This plot illustrates the strong effect of spatial memory on group- and population-level dynamics: Here, a shift from an effectively "short" memory (T < 1) to an effectively "long" memory (T > 1) results in an increase in modal group size of roughly two orders of magnitude.

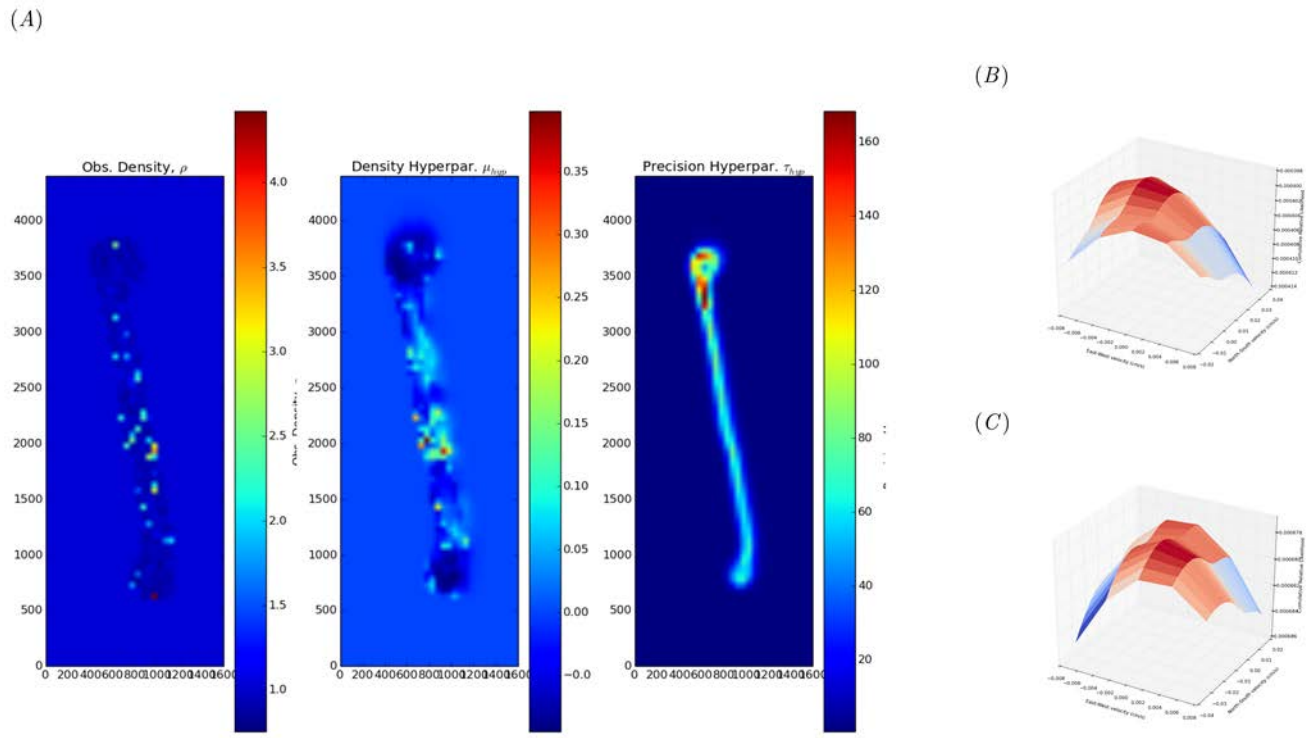

Figure 3 Inferred currents from acoustic survey data, reflecting best fir (likelihood-maximizing) currents in the North-South and East-West directions. (A) Snapshots of acoustic data at 50m depth (left) along with parameters from the Bayesian analysis hyperparameters (middle and right). These hyperparameters represent a log-Normal probability distribution of fish school density at each point in time and space, updated across sparse and irregular samples from the acoustic transects and inferred via dynamic modeling between observations. (B) Relative likelihood plot of current velocities extracted from the acoustic data at 50m depth. The analysis suggests the most probable currents in the 50m depth stratum were approximately 1.6 cm/s to the North and 0.4 cm/s to the West. (C) 1.3 cm/s due South.

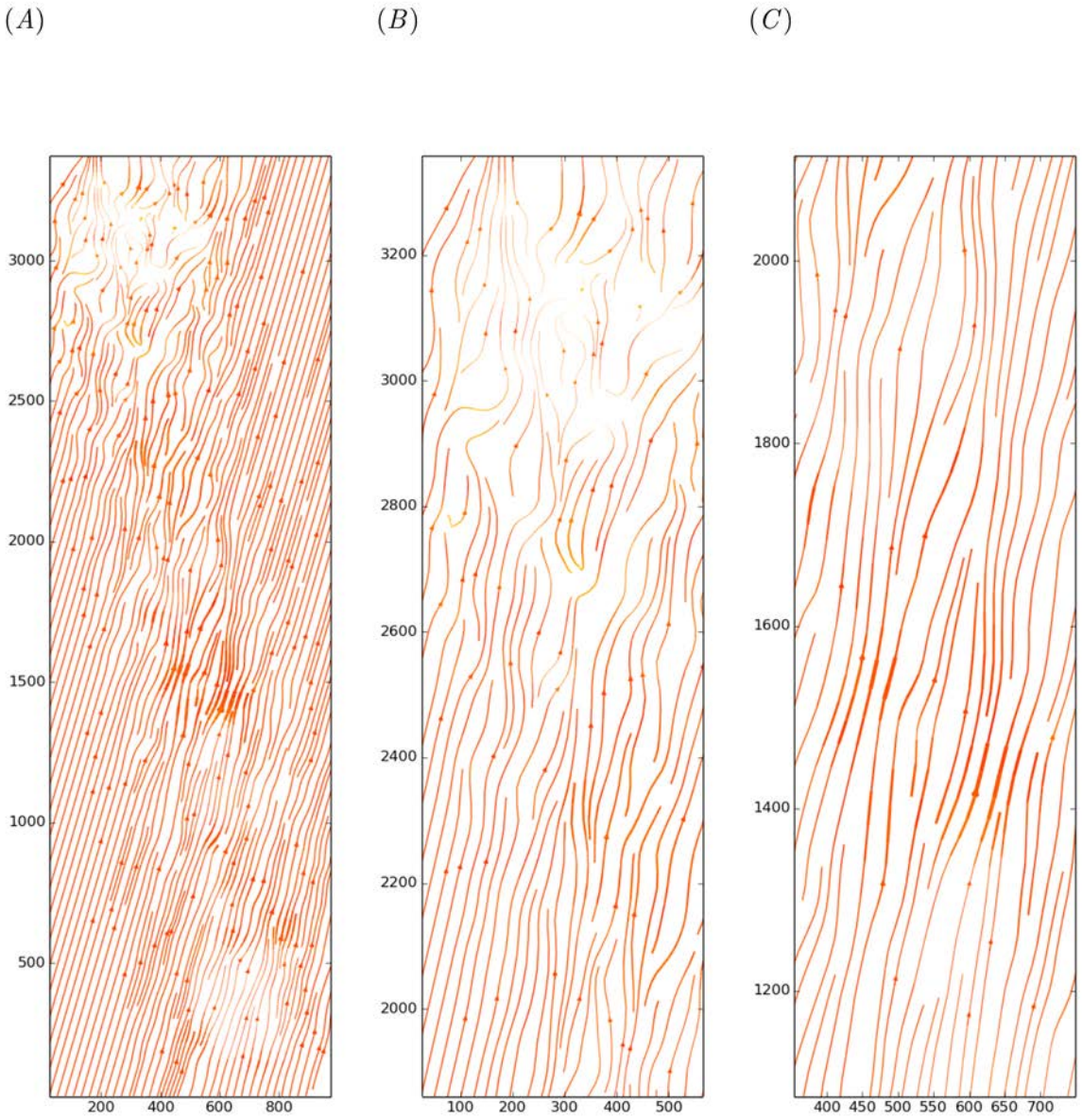

Figure 4 Inferred velocities of Alaskan walleye pollack schools from acoustic survey data. In these plots, best fit fish group velocities are represented as streamlines, with the direction of lines representing "flow" of fish biomass. Line color reflects best fit estimates of instantaneous swimming speed, and line width represents the "flux" (speed x density) of fish biomass. (A) The entire domain of analysis at the end of the last transect. (B) A zoomed-in view of inferred finescale movements at the upper left of the domain. (C) A zoomed-in view of inferred finescale movements at the middle of the domain. Note that data are more recent in the area represented in (B), yielding a more detailed estimate of school movements than in other regions where uncertainty has accumulated over long periods in which no samples are available. However, that analysis suggests that the region represented in (C) is likely to remain an area of rapid movements of high-density fish schools.

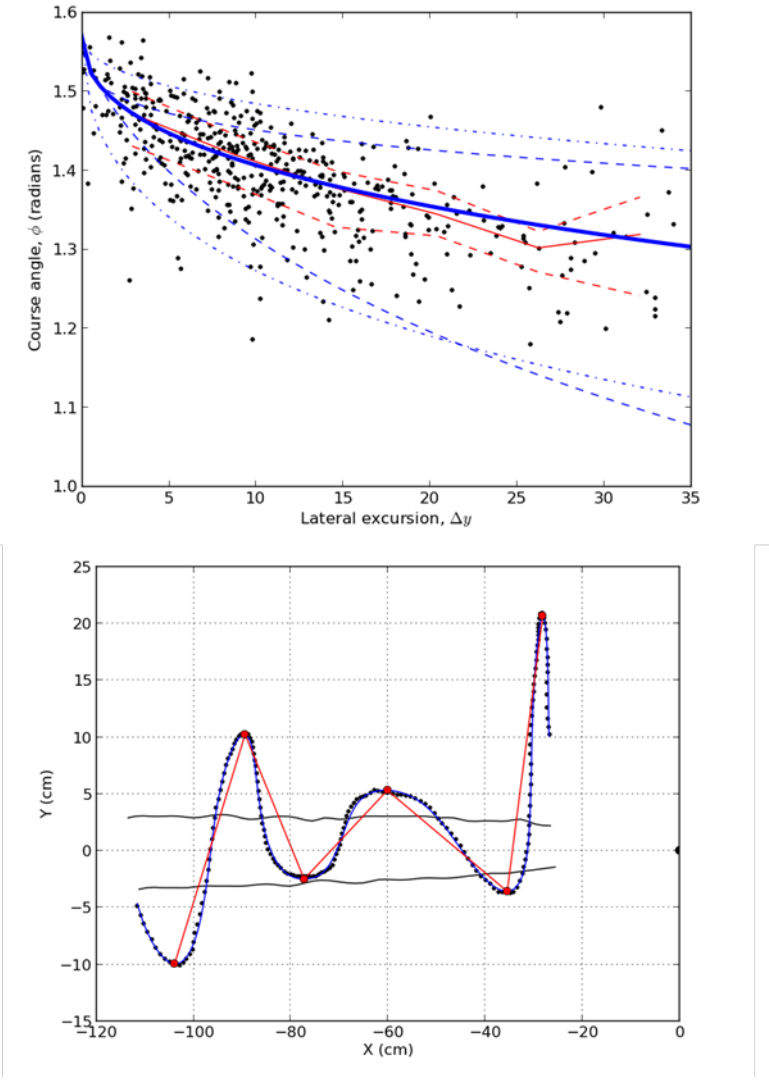

Figure 5. Development of an estimation scheme for cognitive movement behaviors using observed trajectories of a simplified behavior: location of the source of an odorant plume in a turbulent flow. The top plot shows movement of a male moth seeking a pheromone-emitting female, with the odorant source indicated by a black semicircle on the right side. Wind direction is right to left. In this plot, black circles indicate the raw position data; the blue line represents a corrected path after filtering to remove frame rate noise. The red line segments represent straight-line connections between maximum lateral excursions. The bottom plot shows the course angle and lateral excursion of 458 cross-plume transits, aggregated from four flights by each of by 19 moths. The observed data are summarized by the median (solid red line) and 25th and 75th percentiles (dotted red lines). The blue solid line indicates best-fit predictions of a cognitive behavioral model ($p<<0.01$, $r^2=0.43$); dotted blue lines represent a sensitivity analysis for these predictions. These results indicate the methods and results being pursued to estimate fish schooling behavioral parameters from acoustic survey data. From Grünbaum and Willis (2014).

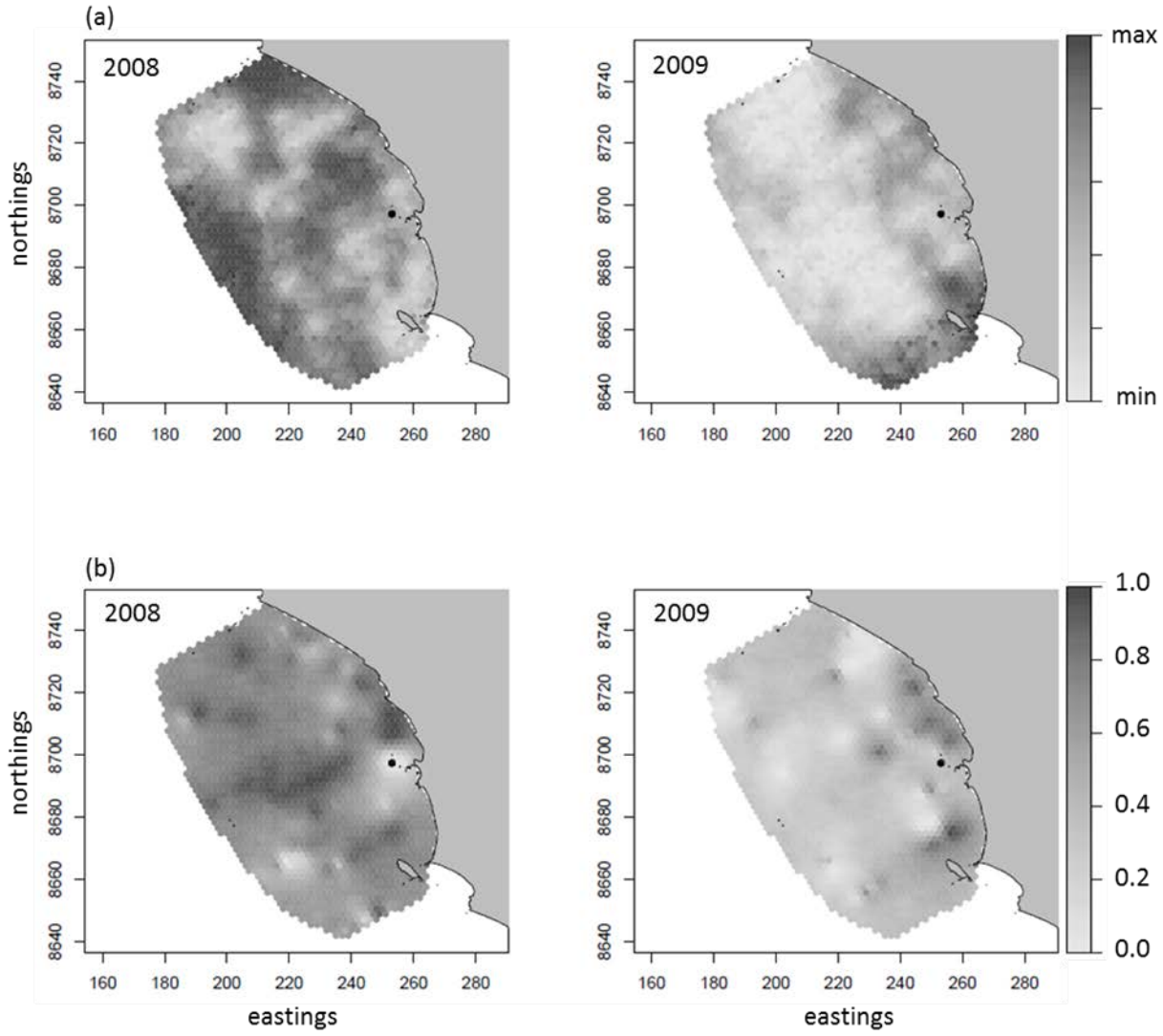

Figure 6. Contrasting foraging conditions in 2008 and 2009. Plots show Bayesian posterior predictions generated from acoustic survey data on anchoveta: (a) mean relative abundance in each cell by quantile; (b) mean probability that the upper depth limit of aggregations is less than 7.412 m, the scaling parameter in the patch selection decision rule for Peruvian Boobies (see Boyd et al., in press). The colony is indicated by a black hexagon. Land is shown in grey.

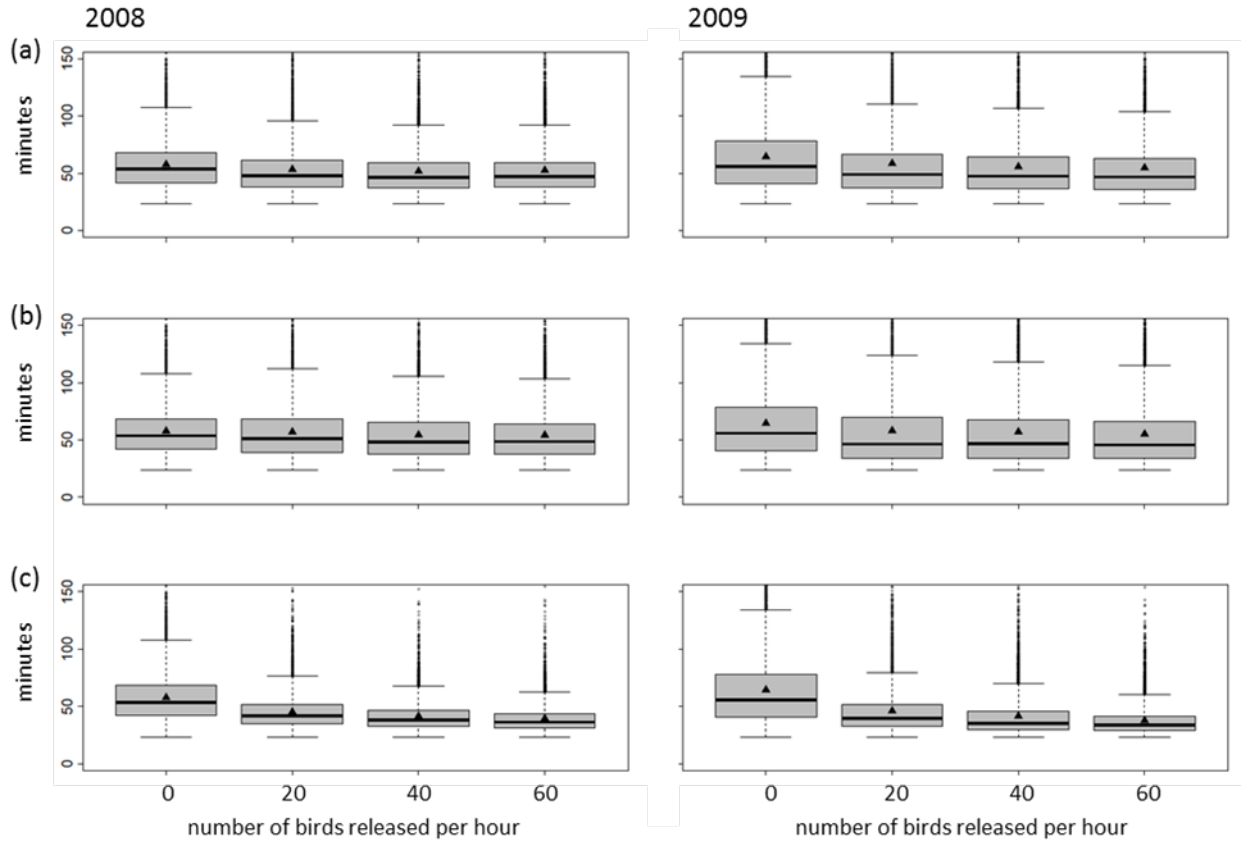

Figure 7. Box plots of foraging trip durations for simulations based on the 2008 and 2009 prey fields with a range of population densities under various information rules: (a) orientation of outbound headings; (b) network foraging; (c) orientation of outbound headings and network foraging. Results for population densities of 0 are derived from the no-information scenario. Mean values are indicated by black triangles.

Sonar imagery of fish schools

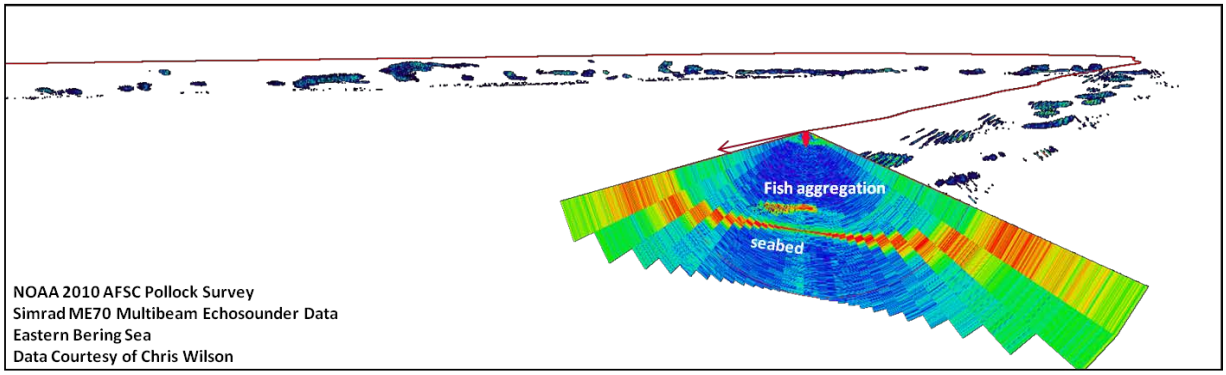

Figure 8. Example of Simrad ME70 multibeam data collected by NOAA-AFSC in the Eastern Bering Sea. A single ping of data representing a 'slice' of the water column is shown in the foreground. Target detections representing aggregations of walleye pollock are shown in the background. The ship's track line is shown in red.

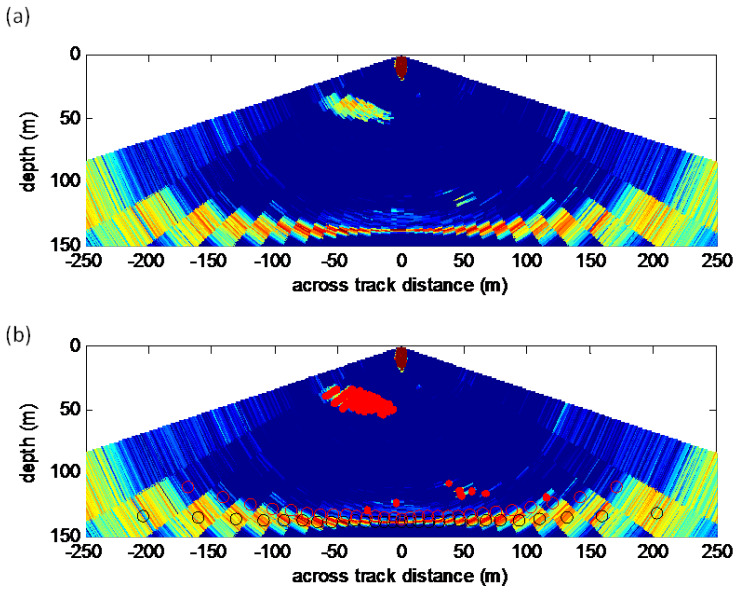

Figure 9. (a) A single raw ping of ME70 MBES data, with a small aggregation of fish located at (-40 m, 40 m). (b) Automatically detected potential fish targets (red dots) after removal of data below the seabed returns (red circles).

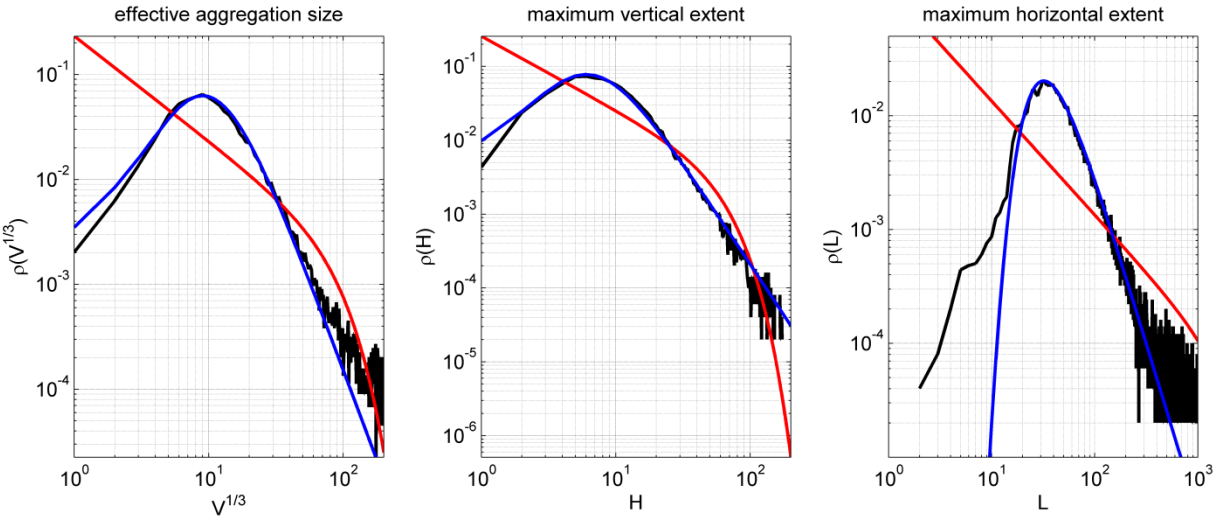

Figure 10. Statistics of fish school dimensions. Black line: Size distributions for effective size, maximum vertical extent, and maximum horizontal extent, as measured by NOAA-AFSC in the Eastern Bering Sea. Red line: Niwa's model. Blue line: Anderson's model. Note that the axes change for each plot.

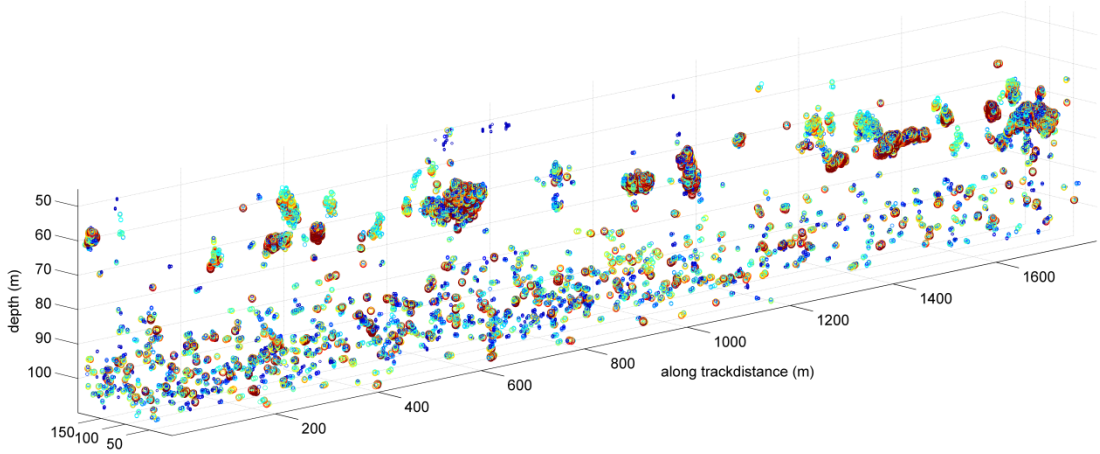

Figure 11. An example transect from the first set of repeat transects (school subset 1) in the Eastern Bering Sea, with dense aggregations of fish ('cherryballs') in the upper 80 m and a loose aggregation of fish below 80 m.

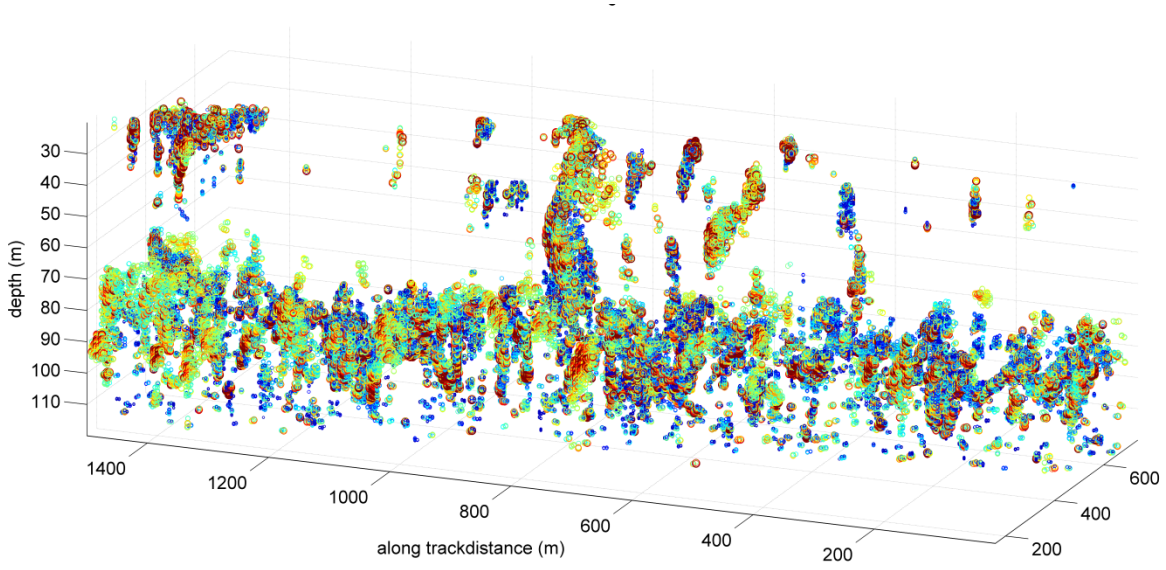

Figure 12. An example transect from the second set of repeat transects (school subset 2) in the Eastern Bering Sea, with dense aggregations of fish found throughout the water column.

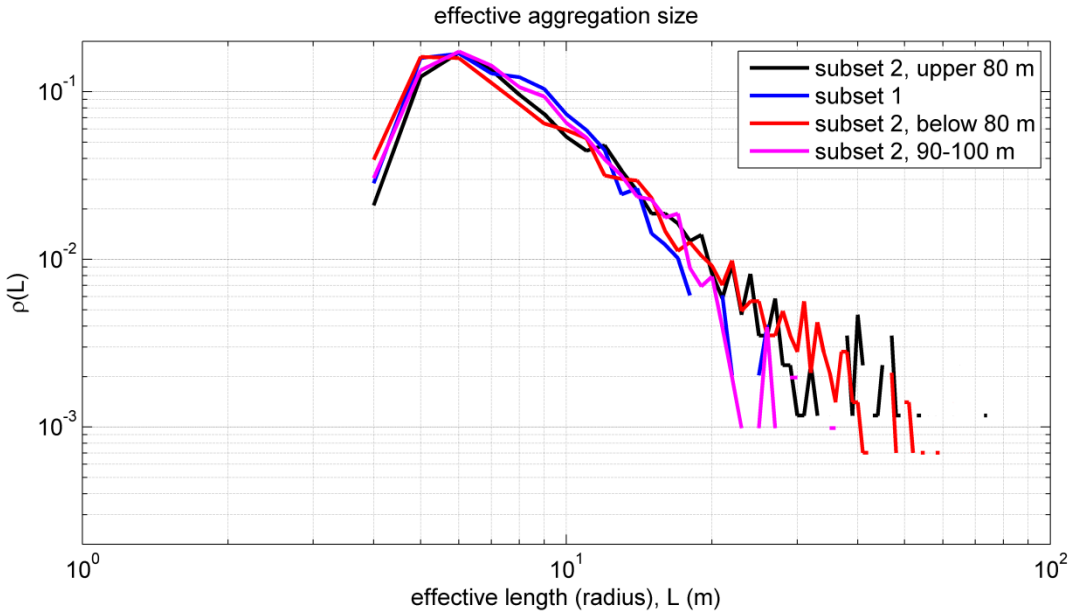

Figure 13. Distributions of effective sizes of fish aggregations (based on Fourier descriptors) were calculated for both subsets of fish data (see legend) from Eastern Bering Sea, and appear similar in all cases. For values beyond the mode, there is a power-law appearance (similar to Figure 10) in all cases, with the possible exception of subset 1.

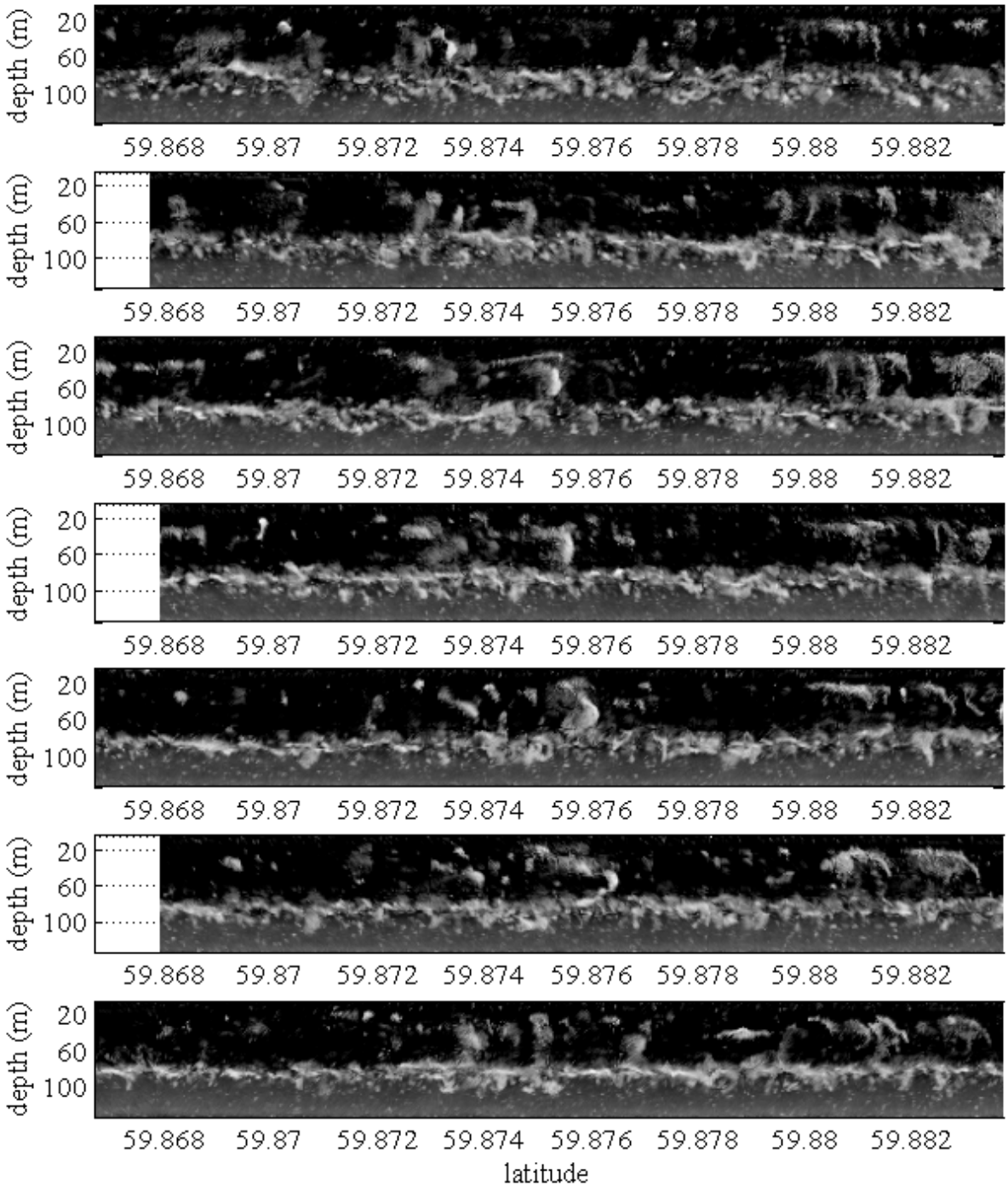

Figure 14. Example synthetic echograms of the ME70 water column data showing the sequential transects in order from top to bottom. The beginning of the first transect (top) occurs at 0559 UTC. The end of the last transect (bottom) occurs at 0737 UTC. The grayscale level corresponds to the volume scattering strength (dB) averaged across-beams in 2 m depth bins.

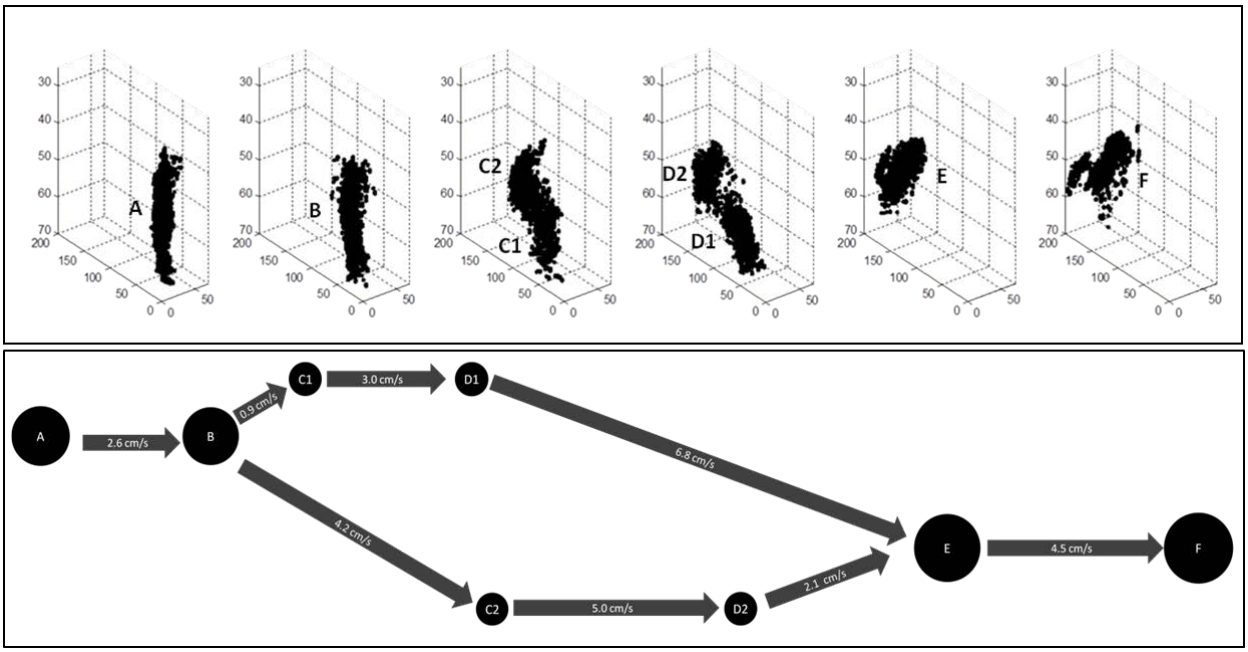

Figure 15. Anatomy of a fission (B to C1/C2) and fusion (D1/D2 to E) event. The upper panel shows raw detections extracted from six subsequent passes over an aggregation of fish with a multibeam echosounder data (5x vertical exaggeration). The lower panel describes the change in aggregation structure from pass to pass. In the lower panel, the size of the circles are proportional to the estimated number of fish, and the length of the arrows are proportional to the distance the school has moved. Data collected by the NOAA Alaska Fisheries Science Center acoustic/trawl walley pollock survey in the Gulf of Alaska, 2012.

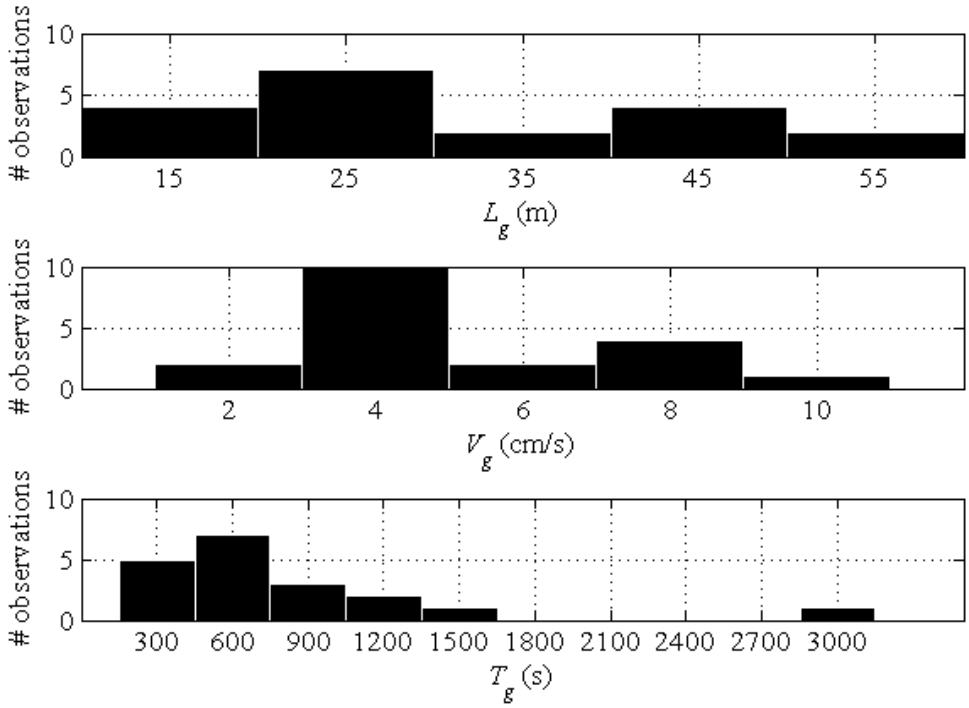

Figure 16. Group length, velocity, and time scales observed from shallow (<75 m) groups that were tracked over at least two subsequent transects.